Mon. Not. R. Astron. Soc. **278,** 773–780 (1996)

Fe XII emission lines in spectra obtained with the *Solar EUV Rocket Telescope and Spectrograph* (*SERTS*)

F. P. Keenan,[1] R. J. Thomas,[2] W. M. Neupert,[2] V. J. Foster,[1] P. J. F. Brown[1] and S. S. Tayal[3]

[1] *Department of Pure and Applied Physics, Queen's University, Belfast BT7 1NN*
[2] *Laboratory for Astronomy and Solar Physics, Code 680, NASA/Goddard Space Flight Center, Greenbelt, MD 20771, USA*
[3] *Department of Physics and Center for Theoretical Studies of Physical Systems, Clark Atlanta University, Atlanta, GA 30314, USA*

Accepted 1995 August 31. Received 1995 August 16; in original form 1995 July 17

ABSTRACT

Many intensity ratios involving Fe XII $3s^23p^3-3s3p^4$ and $3s^23p^3-3s^23p^23d$ transitions in the 186–383 Å wavelength range are known to be sensitive to electron density. We compare calculations for these lines with observations of a solar active region and of a subflare obtained during the 1989 flight of the *Solar EUV Rocket Telescope and Spectrograph* (*SERTS*). Electron densities derived from the majority of such ratios are consistent with one another for both solar features, and are also in good agreement with the values of N_e estimated from diagnostic lines in other species formed at similar electron temperatures to Fe XII, such as Fe XIII and Fe XIV. These results provide observational support for the general accuracy of the diagnostic calculations, and imply that they may be applied to future observations planned with the *Coronal Diagnostic Spectrometer* on the *SOHO* mission. In addition, our analysis indicates that the line at 283.70 Å in the active region data is the $3s^23p^3\ ^2D_{3/2}-3s3p^4\ ^2P_{1/2}$ transition in Fe XII, the first time (to the best of our knowledge) that this line has been identified in the solar spectrum. Five of the line ratios considered are predicted to be relatively insensitive to the adopted electron temperature and density, and the good agreement found between theory and observation for three of these provides evidence for the reliability of the *SERTS* instrument calibration. However, for one of the remaining ratios the large discrepancies between theory and observation cannot be attributed to blending, and may be due to errors in the adopted atomic data.

Key words: atomic data – Sun: activity – Sun: flares – ultraviolet: general.

1 INTRODUCTION

Emission lines arising from $3s^23p^3-3s3p^4$ and $3s^23p^3-3s^23p^23d$ transitions in Fe XII have been frequently observed in solar spectra between ~290–383 and ~186–220 Å, respectively (Kastner & Mason 1978; Vernazza & Reeves 1978; Dere 1982). Dere et al. (1979) noted that the ratios of these lines are very sensitive to electron density, and hence are potentially very useful N_e-diagnostics for the emitting plasma. These authors plotted several theoretical Fe XII line ratios as a function of density, but restricted their results to diagnostics involving either $3s^23p^3-3s3p^4$ or $3s^23p^3-3s^23p^23d$ transitions only. This was primarily because the S082A spectrograph on board *Skylab*, from which Dere et al. obtained their observational data, detected solar spectra in two wavelength settings, namely ~171–330 and ~330–630 Å (Tousey et al. 1977). The relatively uncertain calibration between these two ranges make the measurement of ratios involving lines in both wavelength regions difficult, although not impossible, to determine (see, e.g., Keenan, Widing & McCann 1989).

More recently, the *Solar EUV Rocket Telescope and Spectrograph* (*SERTS*) has obtained solar spectra over the full wavelength range of 170–450 Å in a single exposure (Thomas & Neupert 1994), thereby allowing the development and testing of Fe XII diagnostics involving both $3s^23p^3-3s3p^4$ and $3s^23p^3-3s^23p^23d$ transitions. This is potentially very important for future solar studies, as the Coronal Diagnostic Spectrometer on board the *Solar and Heliospheric Observatory* (*SOHO*) mission, due for launch in

1995, should routinely detect many of the Fe XII EUV lines, which fall within the 150–800 Å wavelength range covered by this instrument (Harrison et al. 1995). In this paper we therefore compare theoretical Fe XII line ratios with the *SERTS* observations, and hence investigate their usefulness as electron density diagnostics.

2 OBSERVATIONAL DATA

The solar spectra analysed in the present paper are those of an active region and a small subflare, recorded on Eastman Kodak 101-07 emulsion by the *SERTS* during a rocket flight on 1989 May 5 at 17:50 UT (Neupert et al. 1992). The observations cover the wavelength region 235.46–448.76 Å in first order and 170–224.38 Å in second order (the short-wavelength cut-off in the latter being due to an absorption edge in the thin aluminium filter installed to reduce stray light), with a spatial resolution of about 7 arcsec (FWHM) and a spectral resolution of better than 80 mÅ (FWHM) in first order and ≤40 mÅ in second order. The active region measurements used here were spatially averaged over the central 4.6 arcmin of the spectrograph slit, whereas the subflare results come from a 22 arcsec portion of the same data set.

The Fe XII transitions identified in the SERTS-89 spectra are listed in Table 1, where we note that we have detected the 196.62 and 283.70 Å lines, which were not listed by Thomas & Neupert (1994) in their summary of the 1989 May 5 observations. The full set of measured parameters for those two new lines in the active region spectrum is given in Table 2. Our tentative identification of the $3s^23p^3\ ^2D_{3/2}$–$3s3p^4\ ^2P_{1/2}$ line at 283.70 Å is of particular importance, as to the best of our knowledege this transition has not previously been detected in solar spectra (see, for example, the line list of Dere 1978, for solar flare spectra obtained with the S082A

Table 2. New Fe XII lines in the SERTS-89 active region spectrum.

Wavelength (Å)	Intensity[1] (erg cm^{-2} s^{-1} sr^{-1})	FWHM (mÅ)
196.618±0.003	346±172	48±11
283.700±0.007	22.5±11.4	61±16

[1]Intensities are based on the revised calibration scale.

Table 1. Fe XII transitions in the 1989 May 5 *SERTS* observations (SERTS-89).

Transition	λ(Å)	R = I(λ)/I(364.46 Å)		Ratio
		Active region[1]	Subflare[2]	designation
$3s^23p^3\ ^2D_{5/2} - 3s^23p^2(^3P)3d\ ^2F_{7/2}$	186.88	5.73+0b[3,4]	1.04+1c	R_1
$3s^23p^3\ ^4S - 3s^23p^2(^3P)3d\ ^4P_{1/2}$	192.37	1.02+1a	1.18+1c	R_{11}
$3s^23p^3\ ^4S - 3s^23p^2(^3P)3d\ ^4P_{3/2}$	193.51	5.49+0b	5.35+0e	R_{12}
$3s^23p^3\ ^4S - 3s^23p^2(^3P)3d\ ^4P_{5/2}$	195.12	5.24+0a	6.62+0d	R_{13}
$3s^23p^3\ ^2D_{5/2} - 3s^23p^2(^1D)3d\ ^2D_{5/2}$	196.62[5]	1.20+0e	–	R_2
$3s^23p^3\ ^2P_{3/2} - 3s^23p^2(^1D)3d\ ^2S$	200.41	1.57+0b	2.93+0c	R_9
$3s^23p^3\ ^2P_{3/2} - 3s^23p^2(^1D)3d\ ^2P_{3/2}$	201.13	1.69+0c	1.48+0e	R_3
$3s^23p^3\ ^2D_{5/2} - 3s^23p^2(^3P)3d\ ^2P_{3/2}$	219.43	5.83–1d	7.77–1e	R_4
$3s^23p^3\ ^2D_{3/2} - 3s3p^4\ ^2P_{1/2}$	283.70[5]	7.85–2d	–	R_8
$3s^23p^3\ ^2D_{5/2} - 3s3p^4\ ^2P_{3/2}$	291.01	4.69–1a	4.42–1e	R_5
$3s^23p^3\ ^2D_{3/2} - 3s3p^4\ ^2D_{3/2}$	335.04	5.59–2d	7.08–2e	R_6
$3s^23p^3\ ^2D_{5/2} - 3s3p^4\ ^2D_{5/2}$	338.27	3.30–1a	5.27–1b	R_7
$3s^23p^3\ ^4S - 3s3p^4\ ^4P_{1/2}$	346.86	2.88–1a	2.72–1b	R_{14}
$3s^23p^3\ ^4S - 3s3p^4\ ^4P_{3/2}$	352.11	6.22–1a	7.54–1a	R_{15}
$3s^23p^3\ ^4S - 3s3p^4\ ^4P_{5/2}$	364.46	1.00+0	1.00+0	–
$3s^23p^3\ ^2P_{3/2} - 3s3p^4\ ^2D_{5/2}$	382.86	3.06–2c	3.38–2e	R_{10}

[1] $I(364.46\ Å) = 288.0 \pm 33.0$ erg cm^{-2} s^{-1} sr^{-1}, based on the revised absolute calibration scale.
[2] $I(364.46\ Å) = 260.0 \pm 35.0$ erg cm^{-2} s^{-1} sr^{-1}, based on the revised absolute calibration scale.
[3] A±B denotes $A \times 10^{\pm B}$.
[4] The letters a, b, c, d and e indicate errors of <20, <30, <40, <50 and >50 per cent, respectively, in the line-ratio measurements.
[5] Line not listed by Thomas & Neupert (1994).

instrument on board *Skylab*). We return to a more complete discussion of the 283.70-Å feature in Section 4.

Intensities of the Fe XII lines were determined by fitting Gaussian profiles to microdensitometer scans of the recorded spectra, as discussed by Thomas & Neupert (1994). The intensities of the 364.46-Å line in the two solar features are listed in Table 1; the observed intensities of the other Fe XII transitions may be inferred from these using the line ratios given in the table (see Section 3). Observational uncertainties in the line ratios, which are mostly <40 per cent (see Table 1), have been determined using methods discussed in detail by Thomas & Neupert. We note that a recent re-evaluation of the absolute calibration scale for SERTS-89 increases all active region intensities by a factor of 1.24 over the values reported by Thomas & Neupert.

The quality of the observational data is illustrated in Figs 1 and 2, where we plot the active region and subflare spectra between 351.8–352.4 and 364.2–364.8 Å, respectively. Also shown for comparison in the figures are SERTS-89 measurements of the quiet Sun in these wavelength ranges, which we note are of too low a quality for reliable Fe XII line ratios to be derived.

3 THEORETICAL RATIOS

The model ion adopted for the calculation of Fe XII emission line intensities consisted of the $3s^23p^3\ ^4S$, ^2D, ^2P; $3s3p^4\ ^4P$, ^2D, ^2P, ^2S; $3s^23p^2(^3P)3d\ ^2P$, $(^3P)3d\ ^4P$, $(^1S)3d\ ^2D$, $(^1D)3d^2D$, $(^1D)3d\ ^2P$, $(^3P)3d\ ^2F$, $(^1D)3d\ ^2S$ and $(^3P)3d\ ^2D$ states, making a total of 29 fine-structure levels. Energies for all these levels were taken from Corliss & Sugar (1982).

Electron impact excitation rates among the $3s^23p^3$ states, calculated using the *R*-matrix method, were obtained from Tayal, Henry & Pradhan (1987), while for those between $3s^23p^3$ and $3s3p^4$, and between $3s^23p^3$ and $3s^23p^23d$, the distorted-wave results of Tayal & Henry (1988) and Flower (1977), respectively, were adopted. Oscillator strengths for allowed and intercombination transitions from $3s^23p^3$ to $3s3p^4$, $3s^23p^2(^3P)3d\ ^2P$, $3s^23p^2(^1S)3d\ ^2D$ and $3s^23p^2(^1D)3d\ ^2D$ levels were taken from Tayal & Henry (1986), the calculations of Flower (1977) and Bromage, Cowan & Fawcett (1978) being used for all other lines.

As has been discussed by, for example, Seaton (1964), proton excitation may be important for fine-structure transitions. However, both Flower (1977) and Feldman, Cohen & Doschek (1983) have shown this process to be negligible for Fe XII, and it has therefore been excluded from the present calculations.

Using the atomic data discussed above, in conjunction with the statistical equilibrium code of Dufton (1977), relative Fe XII level populations and, hence, emission-line strengths were estimated. The following assumptions were made in the calculations: (i) that photoexcitation and de-excitation rates are negligible in comparison with the corresponding collisional rates, (ii) that ionization to and recombination from other ionic levels is slow compared with bound–bound rates, and (iii) that all transitions are optically thin. Further details of the procedures involved may be found in Dufton (1977) and Dufton et al. (1978).

In Figs 3–5 we plot the emission-line ratios

$R_1 = I(186.88\ \text{Å})/I(364.46\ \text{Å})$,
$R_2 = I(196.62\ \text{Å})/I(364.46\ \text{Å})$,
$R_3 = I(201.13\ \text{Å})/I(364.46\ \text{Å})$,
$R_4 = I(219.43\ \text{Å})/I(364.46\ \text{Å})$,
$R_5 = I(291.01\ \text{Å})/I(364.46\ \text{Å})$,
$R_6 = I(335.04\ \text{Å})/I(364.46\ \text{Å})$,
$R_7 = I(338.27\ \text{Å})/I(364.46\ \text{Å})$,
$R_8 = I(283.70\ \text{Å})/I(364.46\ \text{Å})$,

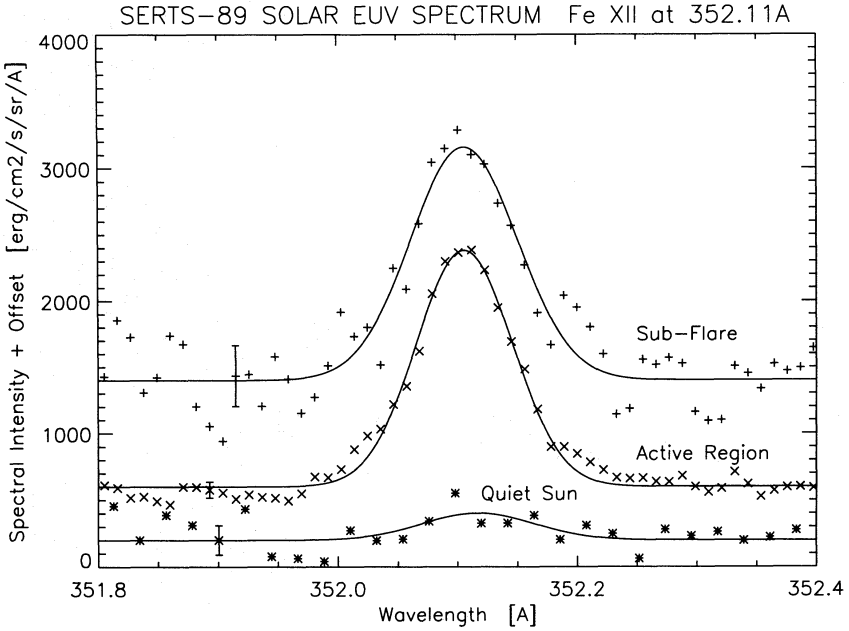

Figure 1. Plot of the SERTS-89 active region and subflare spectra in the wavelength interval 351.8–352.4 Å, containing the Fe XII 352.11-Å line, along with the SERTS-89 measurements of the quiet Sun in this wavelength range. The best-fitting Gaussian profiles to the emission lines are also shown, as is the typical error bar on an observational data point.

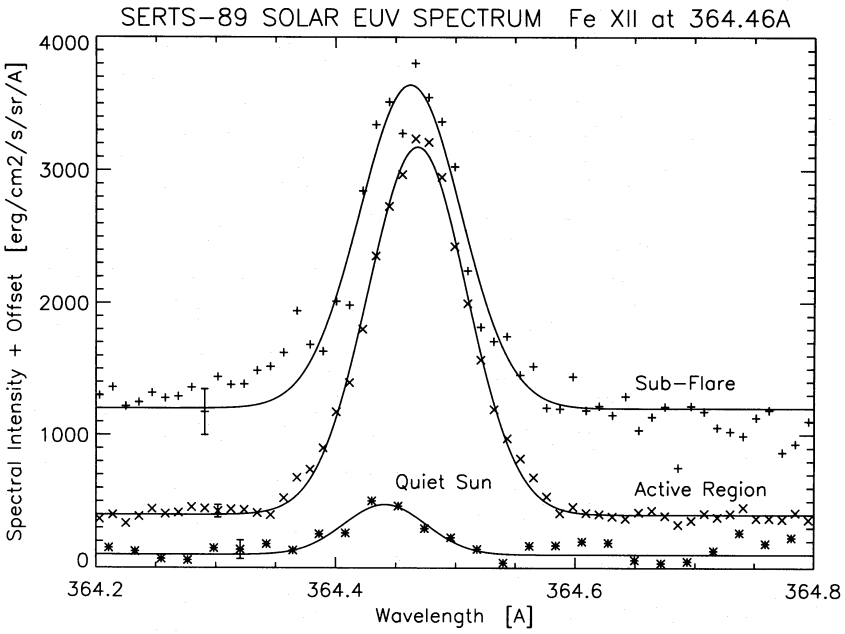

Figure 2. Plot of the SERTS-89 active region and subflare spectra in the wavelength interval 364.2–364.8 Å, containing the Fe XII 364.46-Å line, along with the SERTS-89 measurements of the quiet Sun in this wavelength range. The best-fitting Gaussian profiles to the emission lines are also shown, as is the typical error bar on an observational data point.

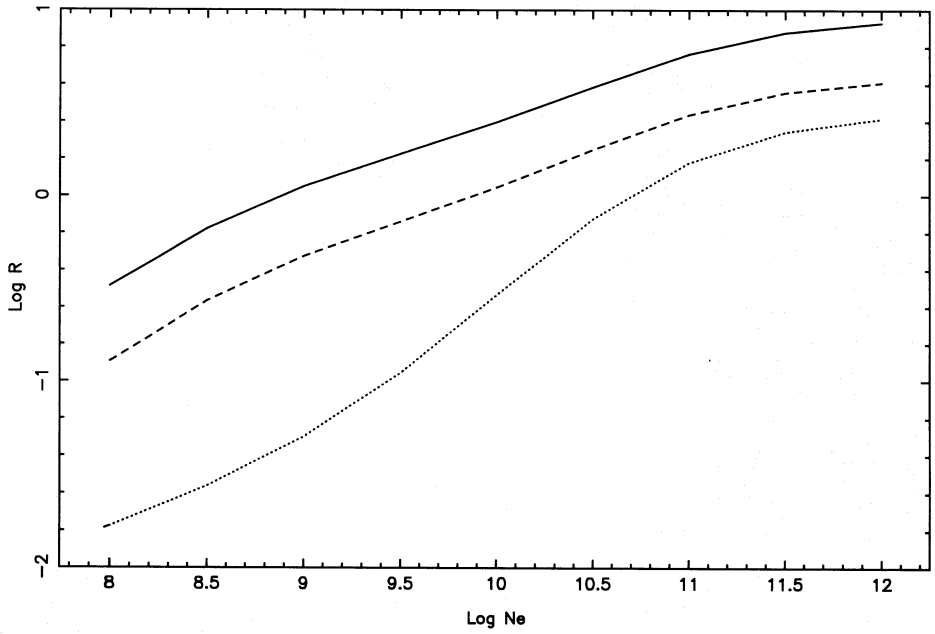

Figure 3. Theoretical Fe XII emission line ratios (line intensities I in energy units), plotted as a function of electron density at the temperature of maximum Fe XII fractional abundance in ionization equilibrium, $T_e = T_{max} = 1.4 \times 10^6$ K (Arnaud & Raymond 1992), with: solid line: $R_1 = I(186.88\ \text{Å})/I(364.46\ \text{Å})$; dashed line: $R_2 = I(196.62\ \text{Å})/I(364.46\ \text{Å})$; dotted line: $R_3 = I(201.13\ \text{Å})/I(364.46\ \text{Å})$.

and

$R_9 = I(200.41\ \text{Å})/I(364.46\ \text{Å})$,

as a function of electron density at the temperature of maximum Fe XII fractional abundance in ionization equilibrium, $T_e = T_{max} = 1.4 \times 10^6$ K (Arnaud & Raymond 1992), although we note that the ratios are relatively insensitive to variations in T_e. For example, reducing the temperature to $T_e = 1.0 \times 10^6$ K leads to changes in R_1 and R_5 of ≤ 10 per cent.

An inspection of Figs 3–5 reveals that the R_1 to R_9 ratios vary significantly with electron density, and hence should be

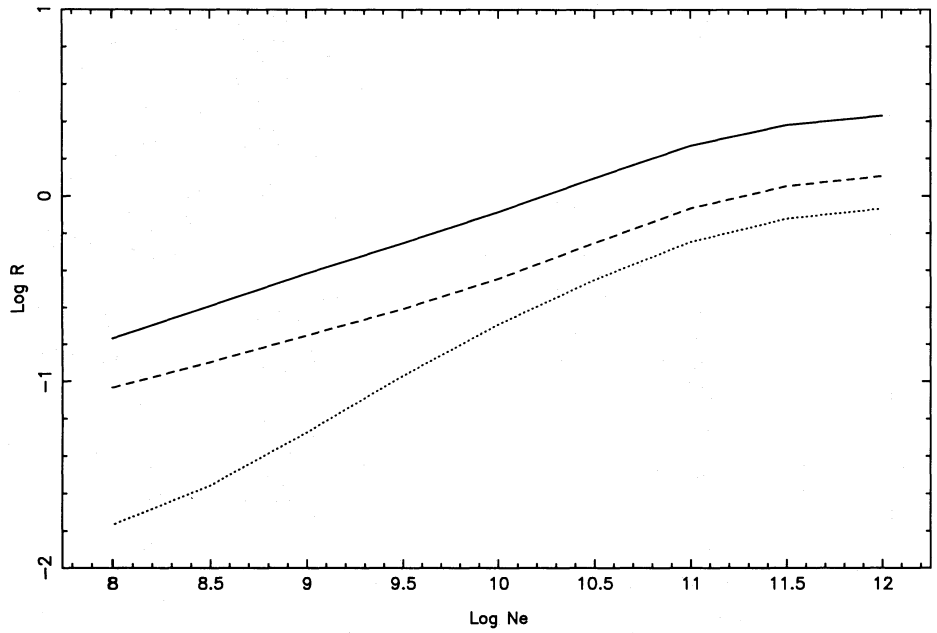

Figure 4. Theoretical Fe XII emission line ratios (line intensities I in energy units), plotted as a function of electron density at the temperature of maximum Fe XII fractional abundance in ionization equilibrium, $T_e = T_{max} = 1.4 \times 10^6$ K (Arnaud & Raymond 1992), with: solid line: $R_4 = I(219.43\ \text{Å})/I(364.46\ \text{Å})$; dashed line: $R_5 = I(291.01\ \text{Å})/I(364.46\ \text{Å})$; dotted line: $R_6 = I(335.04\ \text{Å})/I(364.46\ \text{Å})$.

useful N_e diagnostics. For example, R_2 changes by a factor of ~ 32 between $N_e = 10^8$ and 10^{12} cm^{-3}, while R_6 varies by a factor of ~ 50 over the same density interval.

We note that the ratio

$$R_{10} = I(382.86\ \text{Å})/I(364.46\ \text{Å}),$$

has the same density dependence as R_7 owing to common upper levels, except that

$$R_{10} = 0.187 \times R_7.$$

4 RESULTS AND DISCUSSION

In Table 3 we summarize the electron densities derived by combining observed values of R_1 to R_{10} from Table 1 with calculations from Figs 3–5, where the error bars in log N_e are based on measurement uncertainties. An inspection of the table reveals that the logarithmic electron densities deduced from R_1, R_3 and R_9 in the active region are all ≥ 11.0, which are much higher than those previously estimated for active regions at electron temperatures where the Fe XII lines are formed, $T_{max} = 1.4 \times 10^6$ K. For example, Tayal et al. (1989) estimated log $N_e \simeq 9.8$ from Fe XII line ratios in active regions observed with the S082A spectrograph on board *Skylab*, while Brickhouse, Raymond & Smith (1995) derived log $N_e \simeq 9.5$ for the SERTS-89 active region from line ratios in Fe XIII, which is formed at a similar electron temperature to Fe XII [T_{max}(Fe XIII) $= 1.6 \times 10^6$ K; Arnaud & Raymond 1992]. The very large Fe XII densities deduced here probably arise from overestimates of the relevant line ratios due to blending, a conclusion which is also supported by the fact that R_9 in the subflare is larger than the theoretical high density limit, while R_1 and R_3 in this feature similarly imply unrealistically high values of N_e. In fact, Thomas & Neupert (1994) note that the Fe XII 186.88- and 201.13-Å lines, present in the R_1 and R_3 ratios, are blended with S XI 186.88 Å and Fe XIII 201.13 Å, respectively. Similarly, the Fe XII 200.41-Å line in the R_9 ratio is probably blended with Ca VI 400.83 Å in first order (Kelly 1987). Although in principle it might be possible to estimate the contamination level arising from the blending species by comparison with other observed lines of the ions involved, in practice this is not feasible due to both a lack of suitable features in the spectra and the large sensitivity the theoretical line intensities have to the adopted electron temperature and density.

Electron densities deduced from the remaining Fe XII line ratios in Table 3 are consistent, with discrepancies of typically ≤ 0.3 dex, giving mean values of $\overline{\log N_e} = 9.7 \pm 0.4$ and 9.9 ± 0.5 for the active region and subflare, respectively. These mean densities are in excellent agreement with the values determined from diagnostic ratios in species formed at similar temperatures to Fe XII. For example, as noted above, Brickhouse et al. (1995) found log $N_e \simeq 9.5$ for the active region from Fe XIII, while for the subflare we derive log $N_e \simeq 9.5$ from the $I(219.12\ \text{Å})/I(211.32\ \text{Å})$ and $I(219.12\ \text{Å})/I(220.08\ \text{Å})$ ratios in Fe XIV (Keenan et al. 1991), which has $T_{max} = 1.9 \times 10^6$ K (Arnaud & Raymond 1992). These results provide experimental support for the theoretical Fe XII line ratios (and hence the atomic data used in their derivation), and imply that they may be applied in the future to high-resolution observations from the *Coronal Diagnostic Spectrometer* on the *SOHO* mission (Harrison et al. 1995).

The fact that the R_8 ratio leads to an electron density in good agreement with those inferred from the other Fe XII diagnostics confirms our tentative identification of the 283.70-Å feature as $3s^2 3p^3\ ^2D_{3/2}$–$3s 3p^4\ ^2P_{1/2}$ line, although it has been suggested that this transition should be assigned to

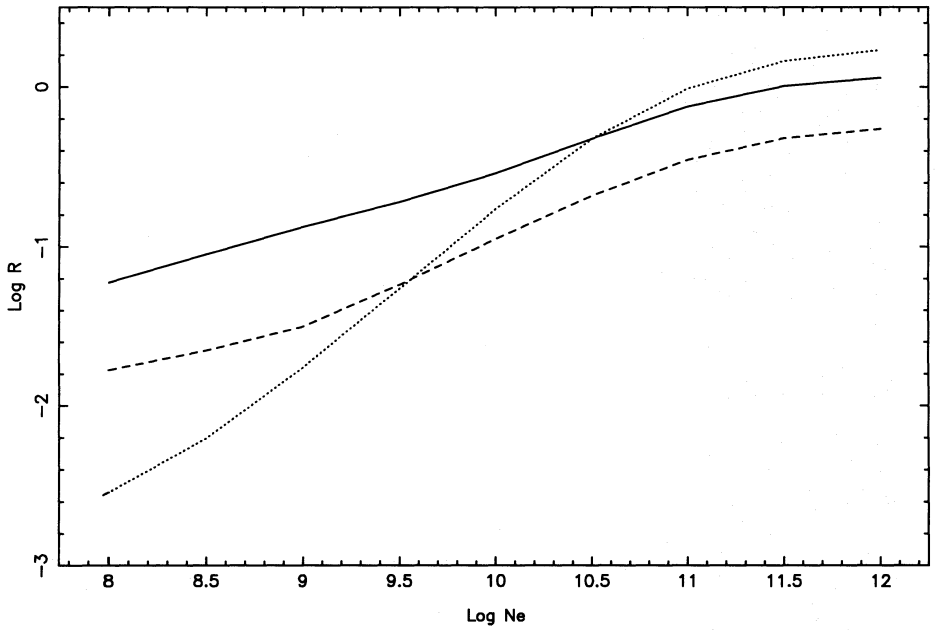

Figure 5. Theoretical Fe XII emission line ratios (line intensities I in energy units, plotted as a function of electron density at the temperature of maximum Fe XII fractional abundance in ionization equilibrium, $T_e = T_{max} = 1.4 \times 10^6$ K (Arnaud & Raymond 1992), with: solid line: $R_7 = I(338.27\ \text{Å})/I(364.46\ \text{Å})$; dashed line: $R_8 = I(283.70\ \text{Å})/I(364.46\ \text{Å})$; dotted line: $R_9 = I(200.41\ \text{Å})/I(364.46\ \text{Å})$.

Table 3. Fe XII logarithmic electron densities.

Ratio	Log N_e(R)	
	Active region	Subflare
R_1	11.0±0.3[1]	≥11.3[1]
R_2	10.1±0.6	–
R_3	11.2±0.4[1]	11.0±0.6[1]
R_4	9.6±0.6	10.2±0.8
R_5	10.3±0.2	10.2±0.8
R_6	9.0±0.4	9.2±0.6
R_7	10.1±0.2	10.6±0.3
R_8	9.7±0.4	–
R_9	≥11.2[1]	H[1,2]
R_{10}	9.3±0.4	9.4±1.3
Mean density[3]	9.7±0.4	9.9±0.5

[1]Affected by known blend.
[2]Indicates that the observed ratio is larger than the theoretical high density limit.
[3]Average density excluding results from the R_1, R_3 and R_9 ratios.

the unidentified line at 283.49 Å. However, the revised intensity of that line, $I(283.49\ \text{Å}) = 79.6 \pm 21.0$ erg cm^{-2} s^{-1} sr^{-1}, would then imply an experimental $R_8 = 0.276 \pm 0.078$, and hence an electron density from Fig. 5 of $\log N_e = 10.8 \pm 0.3$, much larger than those from the other Fe XII diagnostics. In addition, we note that our wavelength for this transition is in somewhat better agreement with that measured from laboratory spectra, $\lambda = 283.64 \pm 0.05$ Å (Fawcett 1971). An alternative identification for the feature at 283.49 Å may be a blend of the N IV $2s2p^3P$–$2s3d^3D$ transitions at 283.42, 283.46 and 283.57 Å (Feldman et al. 1992). The SERTS-89 active region spectrum between 283.3 and 283.8 Å, containing both the 283.49- and 283.70-Å features, is shown in Fig. 6.

Finally, we note that the line ratios

$R_{11} = I(192.37\ \text{Å})/I(364.46\ \text{Å})$,
$R_{12} = I(193.51\ \text{Å})/I(364.46\ \text{Å})$,
$R_{13} = I(195.12\ \text{Å})/I(364.46\ \text{Å})$,
$R_{14} = I(346.86\ \text{Å})/I(364.46\ \text{Å})$,

and

$R_{15} = I(352.11\ \text{Å})/I(364.46\ \text{Å})$,

are predicted to be relatively insensitive to the adopted plasma parameters (temperature and density), and hence may be useful in investigating either blending or the reliability of the instrument calibration (Neupert & Kastner 1983). The observed values of R_{11} to R_{15} are therefore summarized in Table 4, along with the calculated ratios at $T_e = T_{max} = 1.4 \times 10^6$ K, $N_e = 10^{10}$ cm^{-3}, although we note that variations in T_e and N_e of factors of 2 and 10, respectively, lead to a ≤5 per cent change in the theoretical results. An inspection of the table reveals excellent agreement

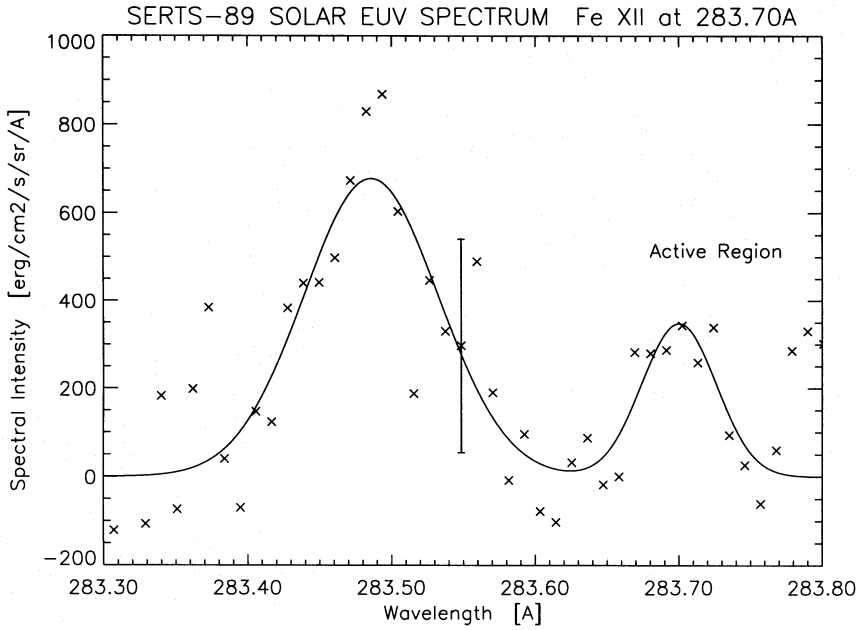

Figure 6. Plot of the SERTS-89 active region spectrum in the wavelength interval 283.3–283.8 Å, showing the emission lines at 283.49 and 283.70 Å. We believe the latter to be the Fe XII $3s^2 3p^3\ ^2D_{3/2}$–$3s3p^4\ ^2P_{1/2}$ transition, while the former may be a blend of the N IV $2s2p^3P$–$2s3d^3D$ lines. The best-fitting Gaussian profiles to the emission lines are also shown, as is the typical error bar on an observational data point.

Table 4. Fe XII density insensitive ratios.

Ratio	Observed		Theoretical[1]
	Active region	Subflare	
R_{11}	10.2	11.8	2.55
R_{12}	5.49	5.35	6.78
R_{13}	5.24	6.62	11.2
R_{14}	0.288	0.272	0.367
R_{15}	0.622	0.754	0.699

[1]Ratios calculated for $N_e = 10^{10}$ cm^{-3}; $T_e = T_{max} = 1.4 \times 10^6$ K (Arnaud & Raymond 1992).

between theory and observation for R_{12}, R_{14} and R_{15}, with discrepancies that average <20 per cent. This is well within the experimental uncertainties in the ratios (see Table 1), and hence once again provides support for the theoretical results. Additionally, as R_{12} contains the 364.46- and 193.51-Å transitions, measured in first and second order, respectively, the good agreement also provides verification of the *SERTS* instrument calibration between the two orders. However, agreement between theory and observation for R_{11} and R_{13} is very poor, with the experimental values for the former being factors of 4 to 5 larger than theory predicts, while for the latter the measured ratios are only about 50 per cent of the theoretical one. Both of these discrepancies are much larger than the observational errors in the ratios (see Table 1). The disagreements for R_{11} are understandable, as the 192.37-Å line is blended with Mn XV 384.75 Å in first order (Thomas & Neupert 1994), but blends with 195.12 Å cannot be possible for the R_{13} problem, as the ratio is smaller than theory predicts. Errors in the instrument calibration are also unlikely, as good agreement is found for other ratios, such as R_{12} (see above). The active region data of Dere (1982), obtained with the S082A spectrograph on board *Skylab*, provide no useful clues, as R_{13} in these observations ranges from ~2.7 to 18.6. (In any event, the S082A results may be unreliable, as the 195.12- and 364.46-Å lines were measured from different plates.) Uncertainties in the theoretical line ratios must be considered a possibility, although we note that Monsignori-Fossi (1992, private communication) also found a similar discrepancy for R_{13} using her Fe XII diagnostics, which have been calculated independently. Clearly, more theoretical work on the Fe XII spectrum is needed, as are better quality observations of solar active regions around the 195.12-Å line.

ACKNOWLEDGMENTS

VJF is grateful to PPARC for financial support. This work was supported by NATO travel grant CRG.930722 and the Royal Society. SST is supported by the US Air Force Office of Scientific Research. The *SERTS* rocket programme was funded under NASA RTOP 879-11-38.

REFERENCES

Arnaud M., Raymond J. C., 1992, ApJ, 398, 394
Brickhouse N. C., Raymond J. C., Smith B. W., 1995, ApJS, 97, 551
Bromage G. E., Cowan R. D., Fawcett B. C., 1978, MNRAS, 183, 19

Corliss C., Sugar J., 1982, J. Phys. Chem. Ref. Data, 11, 135
Dere K. P., 1978, ApJ, 221, 1062
Dere K. P., 1982, Solar Phys., 77, 77
Dere K. P., Mason H. E., Widing K. G., Bhatia A. K., 1979, ApJS, 40, 341
Dufton P. L., 1977, Comp. Phys. Commun., 13, 25
Dufton P. L., Berrington K. A., Burke P. G., Kingston A. E., 1978, A&A, 62, 111
Fawcett B. C., 1971, J. Phys. B, 4, 1577
Feldman U., Cohen L., Doschek G. A., 1983, ApJ, 273, 822
Feldman U., Mandelbaum P., Seely J. F., Doschek G. A., Gursky H., 1992, ApJS, 81, 387
Flower D. R., 1977, A&A, 54, 163
Harrison R. A. et al., 1995, Solar Phys., in press
Kastner S. O., Mason H. E., 1978, A&A, 67, 119
Keenan F. P., Widing K. G., McCann S. M., 1989, ApJ, 338, 563
Keenan F. P., Dufton P. L., Boylan M. B., Kingston A. E., Widing K. G., 1991, ApJ, 373. 695
Kelly R. L., 1987, J. Phys. Chem. Ref. Data, 16, 1371
Neupert W. M., Kastner S. O., 1983, A&A, 128, 181
Neupert W. M., Epstein G. L., Thomas R. J., Thompson W. T., 1992, Solar Phys., 137, 87
Seaton M. J., 1964, MNRAS, 127, 191
Tayal S. S., Henry R. J. W., 1986, ApJ, 302, 200
Tayal S. S., Henry R. J. W., 1988, ApJ, 329, 1023
Tayal S. S., Henry R. J. W., Pradhan A. K., 1987, ApJ, 319, 951
Tayal S. S., Henry R. J. W., Keenan F. P., McCann S. M., Widing K. G., 1989, ApJ, 343, 1004
Thomas R. J., Neupert W. M., 1994, ApJS, 91, 461
Tousey R., Bartoe J.-D. F., Brueckner G. E., Purcell J. D., 1977, Appl. Opt., 16, 870
Vernazza J. E., Reeves E. M., 1978,ApJS, 37, 485